Biogeosciences, 14, 2611–2626, 2017
www.biogeosciences.net/14/2611/2017/
doi:10.5194/bg-14-2611-2017

Biogeosciences Open Access EGU

Flooding-related increases in CO_2 and N_2O emissions from a temperate coastal grassland ecosystem

Amanuel W. Gebremichael[1,2,3], Bruce Osborne[2,3], and Patrick Orr[1,3]

[1]UCD School of Earth Sciences, University College Dublin, Belfield, Dublin 4, Ireland
[2]UCD School of Biology and Environmental Sciences, University College Dublin, Belfield, Dublin 4, Ireland
[3]UCD Earth Institute, University College Dublin, Belfield, Dublin 4, Ireland

Correspondence to: Amanuel W. Gebremichael (amanuel.gebremichael@ucdconnect.ie)

Received: 30 November 2016 – Discussion started: 3 January 2017
Revised: 10 April 2017 – Accepted: 17 April 2017 – Published: 23 May 2017

Abstract. Given their increasing trend in Europe, an understanding of the role that flooding events play in carbon (C) and nitrogen (N) cycling and greenhouse gas (GHG) emissions will be important for improved assessments of local and regional GHG budgets. This study presents the results of an analysis of the CO_2 and N_2O fluxes from a coastal grassland ecosystem affected by episodic flooding that was of either a relatively short (SFS) or long (LFS) duration. Compared to the SFS, the annual CO_2 and N_2O emissions were 1.4 and 1.3 times higher at the LFS, respectively. Mean CO_2 emissions during the period of standing water were 144 ± 18.18 and 111 ± 9.51 mg CO_2–C m^{-2} h^{-1}, respectively, for the LFS and SFS sites. During the growing season, when there was no standing water, the CO_2 emissions were significantly larger from the LFS (244 ± 24.88 mg CO_2–C m^{-2} h^{-1}) than the SFS (183 ± 14.90 mg CO_2–C m^{-2} h^{-1}). Fluxes of N_2O ranged from -0.37 to 0.65 mg N_2O–N m^{-2} h^{-1} at the LFS and from -0.50 to 0.55 mg N_2O–N m^{-2} h^{-1} at the SFS, with the larger emissions associated with the presence of standing water at the LFS but during the growing season at the SFS. Overall, soil temperature and moisture were identified as the main drivers of the seasonal changes in CO_2 fluxes, but neither adequately explained the variations in N_2O fluxes. Analysis of total C, N, microbial biomass and Q_{10} values indicated that the higher CO_2 emissions from the LFS were linked to the flooding-associated influx of nutrients and alterations in soil microbial populations. These results demonstrate that annual CO_2 and N_2O emissions can be higher in longer-term flooded sites that receive significant amounts of nutrients, although this may depend on the restriction of diffusional limitations due to the presence of standing water to periods of the year when the potential for gaseous emissions are low.

1 Introduction

The frequency of flooding events has increased in Europe in the last 3 decades and is likely to increase further in a warmer climate as a consequence of climate change (Beniston et al., 2007; Christensen and Christensen, 2007). It is recognised that flooding could have significant implications for greenhouse gas (GHG) emissions, for example, due to water acting as a barrier to gaseous diffusion, as well as via alterations to soil biological and physio-chemical processes (Hansen et al., 2014; Peralta et al., 2013). Recent studies on the impact of longer-term flooding (LFS) have attributed differences in GHG emissions to a range of factors, including nutrient availability (Juutinen et al., 2001; Samaritani et al., 2011), soil microbial activity (Unger et al., 2009; Peralta et al., 2013), oxygen concentration (McNicol and Silver, 2014) and vegetation characteristics (Lewis et al., 2014). However, there is less information on short-to-medium-term flooding events and it is unclear how flooding impacts on ecosystems that experience variable periods of inundation. The impact of flooding will also depend on the timing, extent and duration of the period of inundation, as well as on site-related variations in topography and hydrology. The extent of freshwater flooding will also depend on the frequency and magnitude of rainfall events.

The natural topographic and hydrological conditions of many coastal plain or floodplain wetlands increases the pos-

sibility of these ecosystems being rapidly inundated with freshwater following extreme precipitation events or extended periods of rainfall. Episodic flooding is a common feature of these ecosystems, with potential sources of water from inland or marine incursions, although inundation from freshwater sources is probably the more common (Doornkamp, 1998). Many assessments of GHG emissions, and an understanding of the factors that control them, are based on information from ecosystems less prone to flooding episodes. These data may not be directly applicable to coastal areas or floodplains where both the volumes involved and the frequency and duration of water incursions can be high. For example, soil water availability can affect the emissions of CO_2 and N_2O by influencing the rates of C and N mineralisation (Alongi et al., 1999; Noe et al., 2013), but it is less clear how variations in standing water levels influence these processes, although this likely depends on the extent and the duration of inundation (Lewis et al., 2014). Previous studies provide contrasting evidence as to whether soil inundation enhances or impedes organic matter mineralisation. Wilson et al. (2011) and Kim et al. (2015) showed that the rate of organic matter mineralisation can be enhanced after a short hydroperiod (the period of time the soil area was waterlogged), whereas longer inundation periods suppressed decomposition by limiting oxygen supply (Lewis et al., 2014). Flooding generally promotes anaerobic conditions by excluding air from the pore spaces in the soil that would reduce mineralisation of organic matter (Altor and Mitsch, 2008). Despite lower mineralisation rates under these conditions, CO_2 emissions are still possible from anoxic soils (Glatzel et al., 2004). A number of factors, such as the quality and quantity of substrates available for microbial processes, temperature, soil microbial activity and oxidation-reduction potential, potentially impact on the magnitude of CO_2 or N_2O exchange in intermittently flooded ecosystems. High soil organic matter concentrations, in combination with warmer conditions in flooded soil, can enhance CO_2 production (Oelbermann and Schiff, 2008; Kim et al., 2015). When associated with sufficient oxygen, CO_2 emissions in wetlands increase as a result of accelerated organic matter decomposition, whilst CH_4 production decreases because of aerobic methane oxidation (Smith et al., 2003). Although CH_4 is often considered to be the more significant GHG in wet or flooded ecosystems, this may not be the case where there are only temporary hydroperiods (Audet et al., 2013; Batson et al., 2015), where CO_2 fluxes are still likely to dominate the annual budget. Finally, the effect of hydroperiod duration on N_2O fluxes has received less attention. We therefore focussed on N_2O and CO_2 fluxes, which are likely to be the more important in many terrestrial ecosystems.

Denitrification and nitrification are often considered to be the main mechanisms by which N_2O is produced in soil, although denitrification may be the dominant process for the release of N_2O both under aerobic and anaerobic soil conditions (Bateman and Baggs, 2005). Denitrification and increased N_2O production is enhanced by high soil water contents (Machefert and Dise, 2004; Maag and Vinther, 1996), although the frequency and duration of flooding may also be important. In riparian systems, a shorter flooding duration correlated with the highest N_2O emissions, which diminished the longer the period of inundation (Jacinthe et al., 2012). In addition to water availability, temperature is also recognised as an important variable in determining the production and consumption of N_2O and CO_2 via its effects on the metabolic activity of microorganisms and plants (Davidson and Janssens, 2006; Butterbach-Bahl et al., 2013; Kirwan et al., 2014; Kim et al., 2015).

Flooding stimulates changes in the structure of soil microbial communities (Bossio and Scow, 1998; Unger et al., 2009; Wilson et al., 2011) and this, in turn, affects the rate of decomposition of organic material (Van Der Heijden et al., 2008). The extent of any change in microbial biomass (MB) and/or microbial populations could also vary with flooding duration (Rinklebe and Langer, 2006). For example, Wilson et al. (2011) showed significant changes in microbial structure and increases in soil enzymatic activity after short-term (24-day) inundation of floodplain soil. Nevertheless, an increase in microbial activity and GHG emissions as a response to short-term flooding (SFS) is not always found (Unger et al., 2009; Jacinthe, 2015), and the timing as well as the frequency of flooding events may be important in determining both the microbial community change and the associated GHG emissions. Organic substrate availability (via the breakdown of plant litter or the introduction of organic compounds in flowing water) is a key factor regulating the activities of soil microorganisms and the mineralisation and immobilisation of carbon and nitrogen (Badiou et al., 2011; Li et al., 2015). The availability of organic substrates influences the activity of carbon-cycling extracellular enzymes and, as a result, can impact on the rate of CO_2 emissions and potentially other GHGs (Li et al., 2015).

Owing to the episodic nature of flooding events, capturing their impact on GHG emissions is quite challenging and a possible explanation for the lack of data from field studies. Given the projected increase in flooding events, an evaluation of their impact on GHG emissions is clearly required. The identification of sites with flooding potential before flooding events and the establishment of the appropriate measurement protocols are crucial steps required to capture the dynamics of GHG fluxes in response to real flooding events. This would enable the capture of the full pattern of GHG fluxes prior to, during and after a flooding event. In this paper, we assess the impact of freshwater inundation, with different hydroperiods, on CO_2 and N_2O fluxes before, during and after real flooding events in a coastal grassland ecosystem over ~ 2 years. The main objective was to assess the effects of short- and long-term flooding on the dynamics of CO_2 and N_2O fluxes and how this impacts on the annual budgets for each gas. We also evaluate the significance of a number

of soil physical, chemical and biological parameters, which may influence the fluxes of CO_2 and N_2O.

2 Materials and methods

2.1 Site description

The study site (53°05′87″ N, 6°04′07″ W) was situated on a low lying area (∼ 0 m a.s.l.) of coastal grassland that forms part of the East Coast Nature Reserve (ECNR), a portion of the larger coastal wetland complex called the Murrough wetlands on the east coast of Ireland, near Newcastle, County Wicklow (Fig. 1). The site is owned and managed by BirdWatch Ireland, predominantly as a habitat for a wide variety of birds. The grassland area lies between a long drainage ditch that runs in a north–south direction and a shingle beach bordering the Irish Sea. In the past 12 years, restoration methods, including water management, low-intensity grazing and crop planting, have been undertaken to maintain the site. The standing water level varies spatially across the site and fluctuates seasonally in response to rainfall and the water-retaining capacity of the drainage ditch. The site experiences near to complete saturation with localised flooding in autumn and winter but drains and dries out in spring and summer. Despite being located in a coastal area, the ditch water is generally characterized as being freshwater with the majority sourced from the landward side.

Differences in elevation (∼ 20–25 cm vertical height) over the site result in variations in hydrological connectivity between different portions of the grassland and the ditch water system. Initial monitoring of the general area indicated that this resulted in spatial hydroperiodic differences. The site was therefore divided into two areas based on these hydroperiod characteristics. The site on the more elevated ground is characterized by less-frequent and shorter-term flooding whilst the site located at lower elevations becomes inundated seasonally for an extended period during the winter (LFS). The plant community of the SFS is mainly dominated by creeping bent (*Agrostis stolonifera*) (48 %), velvet grass (*Holcus lanatus*) (27 %), hair grass (*Eleocharis acicularis*) (11 %), meadow grass (*Poa*) (10 %) and couch grass (*Elymus repens*) (7 %). The LFS is dominated by grasses and rushes, including common couch grass (*Elytrigia repens*) (80 %), sharp-flowered rush (*Juncus acutiflorus*) (12 %) and curled dock (*Rumex crispus*) (4 %). The mean annual rainfall of the study area is 756 mm (based on data from the Dublin Airport station, 50 km north of our study site; data source: Met Éireann).

2.2 Greenhouse gas measurements

The fluxes of the greenhouse gases, CO_2 and N_2O, were measured using closed chambers. The chambers were made from 16 cm diameter acrylic tubing cut to a length of 23 cm with a flat cap of similar material fitted over the top, with an open base. In order to increase the opacity and reflectivity of the chambers, they were painted dark grey inside and outside and, additionally, their outer surfaces were wrapped in silver duct tape. The chambers were placed on top of collars (∼ 16 cm diameter), with rubber lips around the top, which were inserted into the soil to 5 cm depth. The purpose of the rubber lip was to create a secure seal between the chamber and the collar during measurements. After establishment of the LFS and SFS sites in September 2013, six collars were installed at each site. Individual collars were approximately 6 m apart and the array staggered along two parallel transects. There was a ∼ 12 m buffer zone between the two sites. During the period when the sites were inundated, the same chamber was used for sampling but was inserted into a styrofoam support enabling it to be balanced on top of the collar while floating on the water surface. The collars were also extended to a height of 20 cm by fitting another similar, 15 cm long, tube just before the onset of the flooding period. To prevent the chamber from being displaced by wind during sampling, four thin rods were fixed into the ground around each sampling point to maintain the chamber in position. Sampling of gases was generally undertaken two to four times each month but less frequently in the winter months.

Measurements of the CO_2 and N_2O concentration inside the chamber were made using a photoacoustic gas analyser (PAS) (Innova 1412, Denmark), connected to the chamber using Teflon tubing. The tubes were 6 m long with a 4 mm inner diameter and the inlet and outlet of the PAS connected to two ports on the top of the chamber. For sampling, the chamber was placed over the collar for between 5 and 6 min during which time the gas concentration was analysed five to seven times to complete one sample. Fluxes of CO_2 and N_2O ($mg\,m^{-2}\,h^{-1}$) were calculated using

$$F = (\Delta C/\Delta t)(V/A),$$

where $\Delta C/\Delta t$ is the rate of change in gas concentration inside the chamber during the chamber placement period, which was calculated by fitting a best-fit linear regression line to the flux data versus time; V is the chamber volume ($4.069 \times 10^{-3}\,m^3$); and A is the area bounded by the chamber ($0.016\,m^2$). Fluxes of CO_2 and N_2O were computed if linear regressions produced $r^2 > 0.90$ ($P < 0.05$) for CO_2 and $r^2 > 0.70$ ($P < 0.05$) for N_2O.

Annual CO_2 and N_2O emissions for 18 February 2014–17 February 2015 and 1 May 2014–30 April 2015 were computed for the SFS and LFS by linear interpolation of fluxes for each sampling date. The area under the curve was calculated using the trapezoid rule by integrating the area for each 12-month period. To estimate and compare the contribution of CO_2 and N_2O fluxes to the global warming potential (GWP), N_2O was converted to CO_2 equivalents by multiplying it by 298 (IPCC, 2007).

Values of Q_{10} for CO_2 emissions were computed for the SFS and LFS using the equation $Q_{10} = \exp(\text{slope} \cdot 10)$, where the slope was derived from the regression coefficient

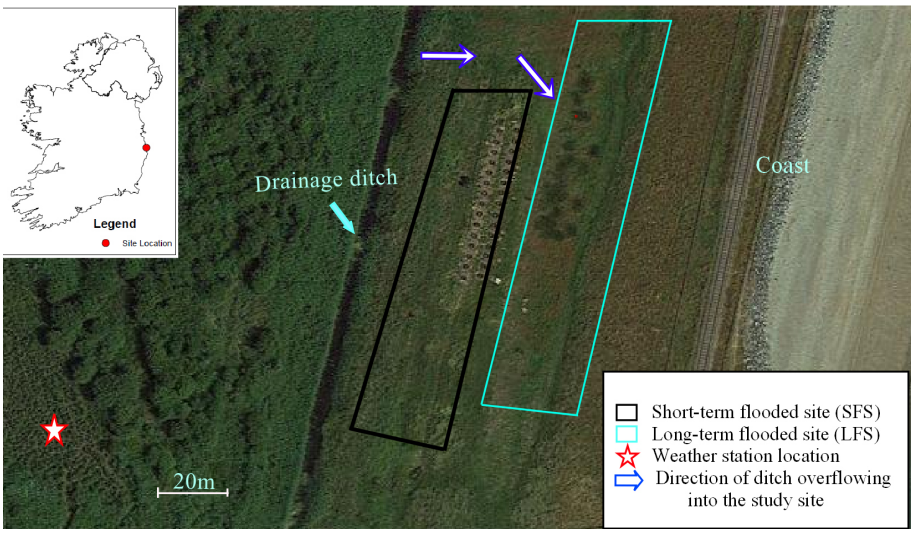

Figure 1. Aerial photograph of part of East Coast Nature Reserve at Blackditch Wood, County Wicklow, showing the study sites and the direction in which water flows during flooding. Inset shows map of Ireland with site location indicated.

of the exponential equation fitted to the CO_2 flux and temperature data.

2.3 Environmental measurements

In addition to the flux measurements, other environmental variables that could potentially influence the GHG fluxes were also measured. A weather station, located about ~ 100 m from the locality where measurements were made, comprised sensors for air temperature (RHT3nl-CA), humidity (RHT3nl-CA), solar radiation (PYRPA-03) and rainfall (RG2 + WS-CA). Average air temperature and cumulative rainfall were recorded at 2 m height every 5 and 60 min, respectively. Soil moisture content and temperature were measured adjacent to the collars/chambers using a handheld ThetaProbe (Delta-T Devices Ltd., Cambridge, UK) each time gas sampling was performed. During the flooding period, the depth of standing water (WD) was measured adjacent to the gas sampling points using a graduated wooden ruler. Redox potential was measured from each collar using a portable Hanna redox meter (HI9125, Hanna Instruments) with a 10 cm redox electrode. Redox potential was measured from the soil surface except when the LFS was flooded above a height of 10 cm, in which case the measurements were acquired from the surface of water. Complete insertion of the electrode to the top soil was avoided to prevent the uncertain impact of the intrusion of water into the electrode through the rim at the top during sampling.

2.4 Biomass determinations

In the summer of 2014, the aboveground plant biomass per unit area was estimated from eight quadrats (45×45 cm) at each site by clipping the vegetation to approximately ground level. Dry biomass was determined after oven drying the fresh samples at 80° C for 72 h.

2.5 Soil sampling for physical and chemical analysis

Sampling of soil from the two sites ($n = 6$ for each site) for analysis of its physicochemical properties was carried out in July 2015 and the samples were then air dried and sieved (2 mm) before analysis. Soil texture was measured using the pipette method (Gee and Bauder, 1986) by first removing the organic content using hydrogen peroxide and then dispersing the samples with sodium hexametaphosphate. Particles were classified as sand (0.063–2 mm), silt (0.002–0.063 mm) and clay (< 0.002 mm). Bulk density was determined by drying each soil sample in a soil core (each 5 cm diameter $\times$ 7 cm height) at 105 °C for 48 h. The density was calculated by dividing the dried soil mass by the core volume. Soil pH was determined on 10 g soil dispersed in 20 mL of deionised water; after 10 min equilibration, a reading was taken using a pH probe/meter (Thermo Fisher Scientific Inc., Waltham, Michigan, USA) while stirring the suspension. Total carbon (TC) and nitrogen (TN) were determined through combustion of finely ground (0.105 mm sieve size) soil using a LECO TruSpec carbon–nitrogen analyser (TruSpec®, LECO Corporation, Michigan, USA). Analysis of TC, TN and pH were performed for samples taken every 5 cm from a 25 cm profile (five samples per sampling point).

Sampling for analysis of NO_3–N and NH_4–N ($n = 4$–6 for each site) was carried out on six occasions from 5 cm depth and an extraction performed by mixing 10 g fresh soil with 2 M KCl. After shaking for 1 h, the KCl extracts were filtered and stored in the freezer until analysis. NO_3–N and NH_4–N were determined from the extracts using an ion anal-

yser (Lachat, QuikChem®, 5600 Lindburgh Drive, Loveland, Colorado, USA)

2.6 Microbial biomass

Microbial biomass C (MBC) and N (MBN) were determined using the chloroform fumigation extraction method (Vance et al., 1987); 10 g samples of fresh soil ($n = 4$–6 for each site) were fumigated in a desiccator with 20 mL ethanol-free chloroform for 72 h and then extracted with 0.5 M K_2SO4. Identical numbers of subsamples were extracted with the same solution but without fumigation the day after sampling. Supernatants from both fumigated and non-fumigated samples were filtered through Whatman no. 1 filter paper and stored in the freezer until analysis. Organic carbon and total nitrogen in the filtrate were analysed using a TOC/TN analyser (Shimadzu, Japan). Estimates of MBC and MBN were derived by calculating the difference between the results of the corresponding fumigated and non-fumigated analysis, divided by the extraction efficiency factor. Factors of 0.45 (Vance et al., 1987) and 0.54 (Brookes et al., 1985) were used for MBC and MBN, respectively, to account for uncompleted extraction of C and N in the microbial cell walls (Jonasson et al., 1996).

2.7 Microbial activity

Soil enzyme/microbial activities were measured from samples ($n = 4$–6 for each site) collected on six sampling occasions (March, August and October 2014; March, May and July 2015). All soil samples were sieved through a 2 mm sieve and analysed in triplicate.

Beta-glucosidase (BG) was determined using the method described by Eivazi and Tabatabai (1988). After placing 1 g of soil in a 50 mL flask, 0.25 mL toluene, 4 mL of modified universal buffer (pH 6.0) and 1 mL β-D-glucoside and p-nitrophenyl-α solutions (PNG) were added sequentially and mixed by swirling. Samples were then incubated at 37 °C for 1 h, following which 1 mL of 0.5 M $CaCl_2$ and 4 mL of 0.1 M of tris(hydroxymethyl)aminomethane (pH 12) were added to halt further reactions. The supernatants were filtered and the absorbance of the filtrate measured at 410 nm using a spectrophotometer (Beckman Coulter, DU 530, UV–vis spectrophotometer). For control samples, the same procedure was followed except that PNG was added just before filtering the soil suspension instead of adding it at the beginning.

Protease activity (PRO) was determined as described by Kandeler et al. (1999). Sodium caseinate (5 mL) solution was added to 1 g soil, and the samples were incubated at 50 °C for 2 h and then filtered after adding 5 mL of trichloroacetic acid solution. Alkali and Folin–Ciocalteu's reagents were added to the filtrates before protease activity was determined colorimetrically at 700 nm.

To determine nitrate reductase (NR) activity, 4 mL of 2, 4-dinitrophenol solution and 1 mL of KNO_3 were added to 5 g samples of soil. After incubation at 25 °C for 24 h, 10 mL 4 M KCl was added and filtered. To 5 mL of the filtrate, NH_4Cl buffer (pH 8.5) sulfanilamide reagent was added, and the activity of the enzyme NR was measured colorimetrically at 520 nm.

Total microbial activity was assayed using fluorescein diacetate (FDA), based on the method described by Schnürer and Rosswall (1982), later modified by Green et al. (2006). Sodium phosphate buffer (pH 7.6) and FDA lipase substrate were added to flasks containing 1 g samples of soil and incubated for 3 h at 37 °C. The fluorescein content in the filtered sample was measured at 490 nm.

2.8 Statistical analysis

All statistical analyses were performed using Minitab 16. All the values reported are means of three to six replicates and standard errors were included when required. To investigate the effects of flooding, we tested for significant differences between the two sites (i.e. the LFS and SFS), for the periods/part periods (A, B, C, D and E) defined on the basis of the state of each site in terms of waterlogging over the study period. This was carried out by applying analysis of variance (ANOVA) for each flux, soil enzymatic activity, TC, TN, mineral N and MB. Functional relationships between potential environmental drivers and the fluxes of CO_2 and N_2O were performed assessed using linear or exponential regression models. Multiple regression analysis was used to determine the relative contribution of more than one independent environmental driver to CO_2 and N_2O fluxes. Normality and homogeneity of the variance of all the models were checked visually from residual versus fitted plots and, when necessary, either square-root or log transformations applied. Differences were considered statistically significant if $P < 0.05$, unless otherwise mentioned.

3 Results

3.1 Soil characteristics

The relative proportion of clay is higher at the LFS, but both sites have sandy loam soil textures. Soil pH was higher at the SFS than the LFS (Table 1). Porosity at the LFS was greater than at the SFS. The soil C and N concentrations were significantly higher ($P < 0.001$) at the LFS site, with the greatest difference in the upper soil layers. At both sites, C and N decreased with soil depth, but more gradually at the SFS (Fig. 2a, b).

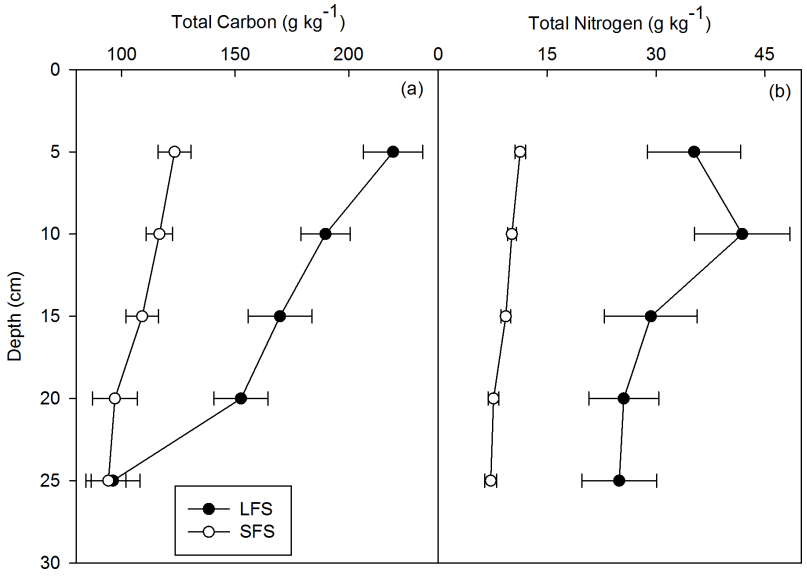

Figure 2. Profile of **(a)** total carbon and **(b)** total nitrogen in the LFS and SFS. Mean values ($n = 6$) are for each level within a profile and the horizontal bars represent the standard errors.

Table 1. Soil properties (0–10 cm) in the LFS and SFS. Values are mean ± SE.

Soil properties	LFS	SFS
Sand (%)	64.40 ± 0.72	69.00 ± 0.95
Clay (%)	16.00 ± 0.44	6.50 ± 0.67
Bulk density (g cm^{-3})	0.73 ± 0.08	1.02 ± 0.04
Porosity	0.73 ± 0.08	0.61 ± 0.04
pH	4.79 ± 0.11	5.28 ± 0.21
Total carbon (g kg^{-1})	204.70 ± 11.90	120.00 ± 6.50
Total nitrogen (g kg^{-1})	38.50 ± 6.52	10.70 ± 0.70
C-to-N ratio	6.79 ± 0.76	10.95 ± 0.15

3.2 Rainfall, water depth, redox potential and air temperature

Depending on the timing and duration of flooding the following periods could be identified, as indicated in Fig. 3: period A was characterized by LFS and SFS flooding, period B by LFS flooding, period C by neither LFS nor SFS flooding, period D by LFS flooding, and period E by neither LFS nor SFS flooding. Thus, there was no equivalent of period A during 2014/2015 (i.e. the SFS was not flooded).

Air temperature followed the seasonal pattern typical for this latitude (Fig. 3a), with the highest values during the summer months (June–August) and the lowest during the winter months (December–February). The values ranged from a high of 23 °C to a low of −3.9 °C with an average of 7.86 °C over the 2-year study period. Rainfall was very variable over the study period (Fig. 3b), with some of the highest rainfall amounts occurring during the warmer months. However, the number of days with rainfall was higher in the cooler period. The mean annual rainfall (866 mm) at our site during the study period was considerably above the average value for the past 30 years (756 mm) measured at the Dublin Airport station.

Standing water was only present at the SFS site for ∼ 1 month (in the winter of 2014) and reached 5 cm depth (Fig. 3c). In contrast, standing water was present for ∼ 6 months at the LFS site in 2015 and reached a depth of ∼ 25 cm in 2014. Whilst standing water at the LFS site was largely associated with the winter periods, it also extended into the spring and autumn periods in 2014/2015 (Fig. 3c).

Variations in soil redox potential broadly correlated with the periods of standing water, with the lowest values occurring in the LFS site in April 2014 and March 2015 (Fig. 3d) reflecting the reducing conditions associated with longer periods of inundation. In contrast, oxidising conditions were always found at the SFS site and these were consistently higher (more positive) than those at the LFS (Fig. 3d). Measurements made from the water column when the LFS was flooded to > 10 cm depth indicated that this was always oxidising and had a low, but positive, redox potential (Fig. 3d).

3.3 Seasonal variations in CO_2 and N_2O fluxes

The results are presented with reference to the periods A–E, which represent the state of the sites in relation to water availability. The CO_2 (Fig. 4a) emissions showed marked seasonal variation, with the highest CO_2 values during the summer months (C, E) at both sites, which correlated with the lowest soil moisture values (Fig. 4c) and the highest soil temperatures (Fig. 4d). The highest CO_2 emissions were observed from the LFS site during each period (C, E) in each

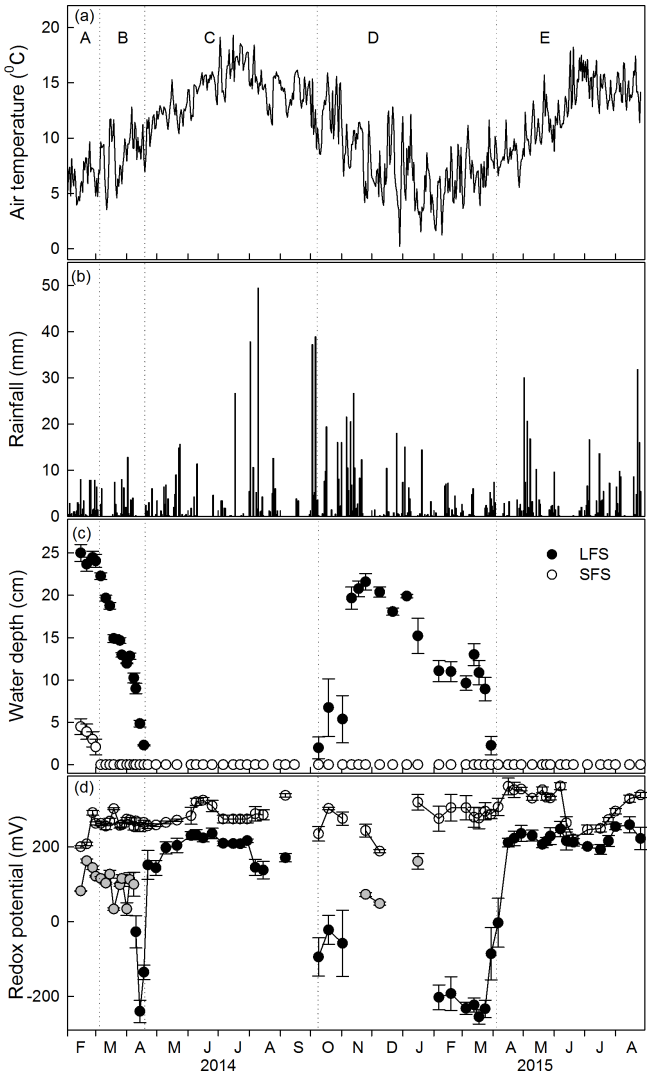

Figure 3. Variations in **(a)** daily air temperature, **(b)** daily rainfall, **(c)** average water depth above the soil surface and **(d)** redox potential at the study sites. Open circles represent redox values from the ground surface of the SFS, black filled circles represent values from the soil surface of the LFS and grey filled circles show values from the water surface while the LFS was flooded to greater than 10 cm depth. Period A: LFS and SFS flooding; period B: LFS flooding; period C: neither LFS nor SFS flooding; period D: LFS flooding; period E: neither LFS nor SFS flooding. Thus, there was no equivalent of period A during late 2014–early 2015.

year and values were higher in 2015, compared to 2014, particularly for the SFS site (Fig. 4a). The lowest emissions were observed during the winter months of both years (A, B, D) when there were no significant differences ($P = 0.768$) between the LFS and SFS sites, even though there was standing water at the LFS site (Fig. 3c).

In period A and the first part of period B, CO_2 emissions are similar for the SFS and LFS. Towards the end of period B the emissions are higher from the LFS, corresponding to the time when the water depth at the LFS was decreasing (Fig. 3c). At the LFS, CO_2 emissions during period C ranged from 16.94 to 498.18 mg CO_2–C m^{-2} h^{-1}, whereas at the SFS, the values ranged from 16.68 to 429 mg CO_2–C m^{-2} h^{-1}. The initial part of period C is characterised by low and similar values of CO_2 emissions for each site that are not appreciably different ($P = 0.956$) from those of the preceding period B. Towards the middle of period C, CO_2 emissions decline and then increase again corresponding to a decrease and then increase in soil moisture. For the June–September 2014 interval within period C, CO_2 emissions from the two sites were significantly different ($P < 0.034$).

In period D, similar trends in CO_2 emissions with time (Fig. 4a) were observed for the two sites despite differences in soil moisture (Fig. 4c) and water depth (Fig. 3c). In period E, CO_2 emissions ranged from 53.32 to 477.26 mg CO_2–C m^{-2} h^{-1} at the LFS and from 55.68 to 343.44 mg CO_2–C m^{-2} h^{-1} at the SFS. As for the corresponding of the previous year (period C), the difference between the two sites was significant ($P = 0.013$) for part of period E (May–August 2015).

Based on the relationships between soil respiration and temperature estimated values for Q_{10} were 2.49 and 2.08 at the LFS and SFS, respectively.

Unlike the CO_2 fluxes, the N_2O emissions generally showed no discernible pattern between seasons during the study period (Fig. 4b) and there were no systematic changes over time. No significant differences ($P > 0.05$) in N_2O fluxes were observed between the LFS and SFS in any of the five periods. In the first wetter periods (periods A and B combined), N_2O fluxes ranged from −0.210 to 0.319 mg N_2O–N m^{-2} h^{-1} and from −0.503 to 0.364 mg N_2O–N m^{-2} h^{-1} at the LFS and SFS, respectively. In period D, the N_2O fluxes from the LFS showed higher variability than those from the SFS, with values between −0.203 and 0.695 mg N_2O–N m^{-2} h^{-1} for the LFS and between −0.307 and 0.206 mg N_2O–N m^{-2} h^{-1} for the SFS. Overall N_2O fluxes were generally higher from the LFS than from the SFS during period D. In the first growing season (period C), the SFS showed consistently higher and more positive N_2O fluxes; the maximum emission recorded (0.651 mg N_2O–N m^{-2} h^{-1}) was, however, from the LFS, at the end of July. N_2O fluxes less than zero suggest uptake of N_2O, which was more common at the SFS site.

Annual CO_2 emissions were 8.18 and 8.76 (mean 8.47) and 11.24 and 11.5 (mean 11.37) Mg CO_2–C ha^{-1} yr^{-1} from the SFS and LFS, respectively, with values for the LFS 1.4 times higher than that from the SFS. For the same years the annual N_2O emissions were 1.3 times higher (7.09 and 5.49 kg N_2O–N ha^{-1} yr^{-1}) from the LFS (mean 6.29) compared to the SFS (5.47 and 3.62 kg N_2O–N ha^{-1} yr^{-1}; mean 4.54).

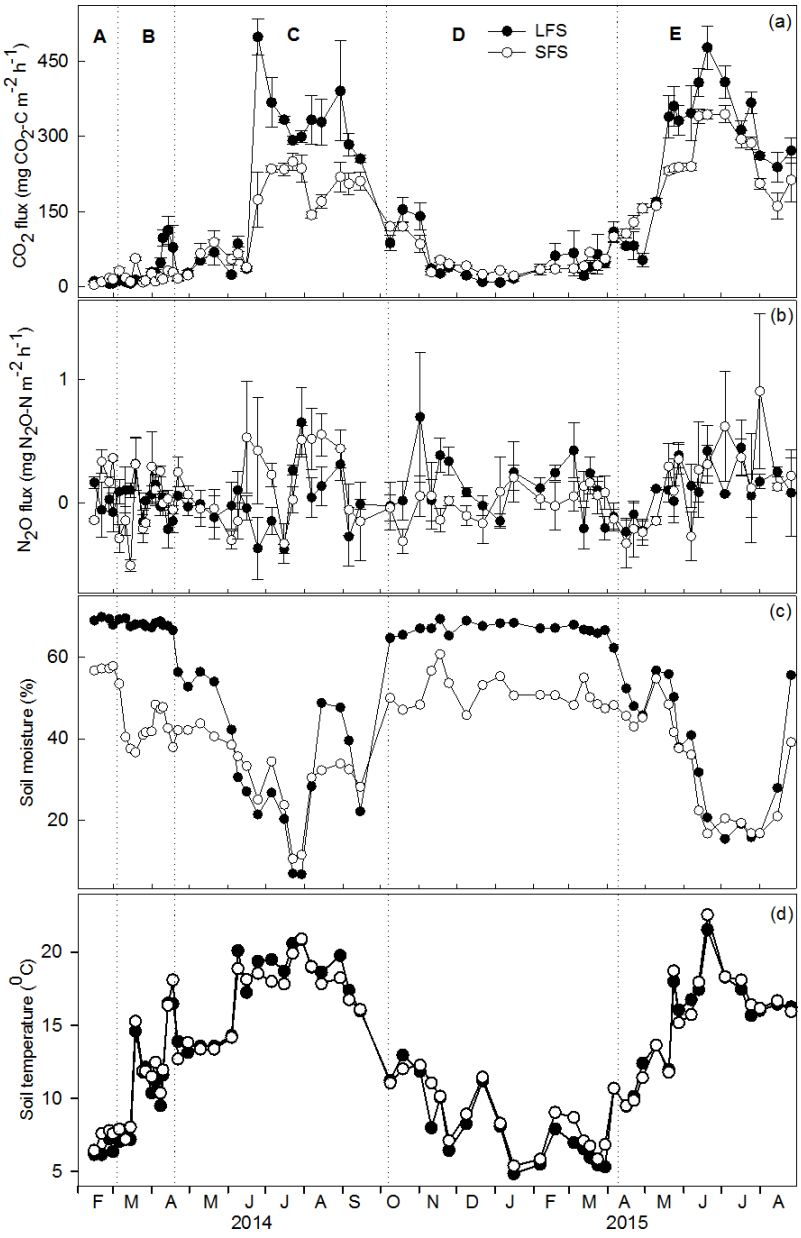

Figure 4. Seasonal variations in **(a)** CO_2 fluxes, **(b)** N_2O fluxes **(c)** soil moisture and **(d)** soil temperature in each site. Periods as defined in Fig. 3.

3.4 Relationship between CO_2 and N_2O fluxes and environmental parameters

Independent testing of the various environmental variables showed that soil temperature, soil water content, redox potential and, for the LFS, water depth were significantly correlated with the CO_2 emissions. Significant positive correlations were found between CO_2 emissions and soil temperature for both the SFS ($R^2 = 0.44$, $P < 0.001$) and LFS ($R^2 = 0.56$, $P < 0.001$), with a stronger relationship at the LFS (Fig. 5a). A significant negative linear relationship between soil moisture and CO_2 emission was found at the LFS ($R^2 = 0.52$, $P < 0.001$) and the SFS ($R^2 = 0.54$, $P < 0.001$) (Fig. 5b). Correlations between CO_2 emissions and redox potential were low, with R^2 values of 0.25 (LFS) and 0.16 (SFS), respectively, but significant at $P < 0.05$. CO_2 emissions at the LFS were exponentially correlated with water depth ($R^2 = 0.45$, $P < 0.001$) (Fig. 5c). Combining soil temperature and soil water content in multiple regression analyses with the CO_2 fluxes only resulted in a small increase in explanatory power to ~ 58 and 66 % at the SFS and LFS, respectively, but including redox potential had no impact on the explanatory power.

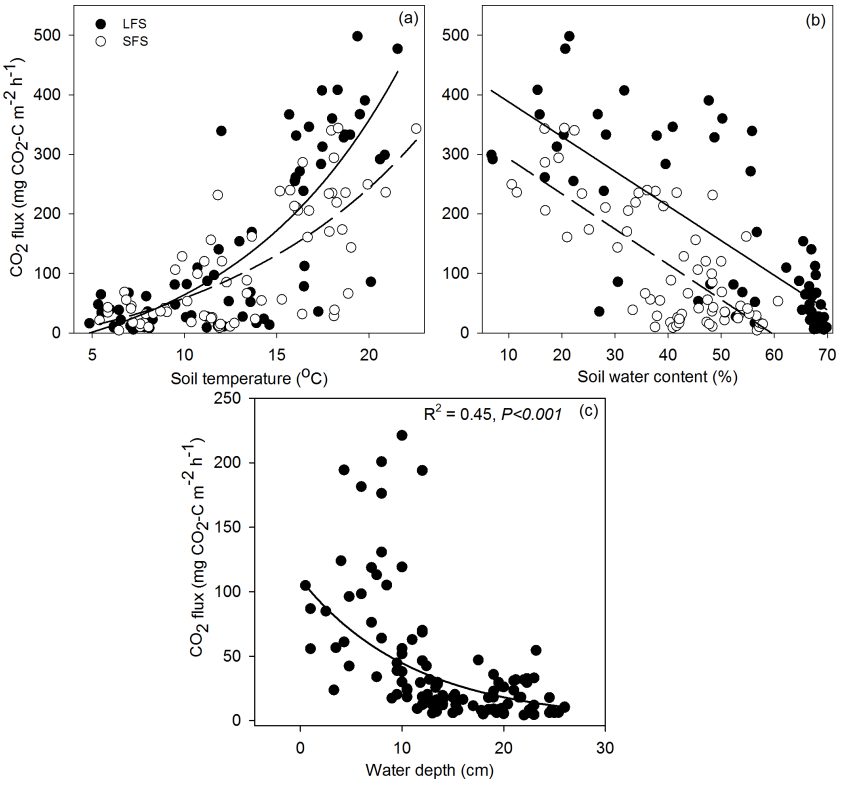

Figure 5. Relationships between CO_2 fluxes and **(a)** soil temperature, **(b)** soil moisture and **(c)** water depth at the LFS. The lines in **(a)** represent the best-fit regression $y = 50.69(\exp 0.09 \cdot T)$, $R^2 = 0.56$, $P < 0.001$ and $y = 53.62(\exp 0.07 \cdot T)$, $R^2 = 0.44$, $P < 0.001$ for the LFS and SFS, respectively. The lines in **(b)** represent the best-fit regression $y = 446.26 - 5.82 \cdot (\mathrm{SWC})$, $R^2 = 0.52$, $P < 0.001$ and $y = 351.95 - 5.92 \cdot (\mathrm{SWC})$, $R^2 = 0.54$, $P < 0.001$ for the LFS and SFS, respectively. The relationship in **(c)** is represented by $y = 109.65(\exp(-0.04 \cdot \mathrm{WD}))$, $R^2 = 0.45$, $P < 0.001$. Values in **(a, b)** are means for $n = 3$–4.

No significant relationship was observed between N_2O fluxes and any of soil temperature, soil moisture, redox potential or water depth at the LFS. At the SFS, soil N_2O fluxes did correlate positively with soil moisture ($R^2 = 0.13$, $P < 0.01$) and soil temperature ($R^2 = 0.13$, $P < 0.01$), but with a low explanatory power. The N_2O flux was not correlated with redox potential at the SFS.

3.5 Soil enzymatic/microbial activity

While there are some significant differences between different sampling dates for BG, FDA and PRO, they, overall, show similar values for, and variation at, both sites (Fig. 6). For period B, BG activity was significantly lower ($P = 0.017$) at the LFS; however, in the second flooding period (first part of period D), BG was significantly higher ($P = 0.001$) at the LFS than at the SFS. In period E, FDA activity was significantly higher ($P = 0.001$) at the LFS than the SFS. In contrast, NR activities were consistently and significantly lower ($P < 0.001$) at the SFS and independent of water status (standing water availability).

3.6 Microbial biomass and soil NO_3^- and NH_4^+

Seasonal variations in MB appear to differ between the LFS and SFS (Fig. 7). Total MBC was generally higher at the LFS than at the SFS at each sampling period, but significant ($P < 0.01$) for periods B, late D and early E (Fig. 7a). MBN values were higher at the LFS than at the SFS (Fig. 7b) for all except two sampling dates. For MBC, MBN ratios were significantly higher ($P < 0.01$) at the LFS during periods of standing water (Fig. 7c).

The concentrations of NH_4^+ and NO_3^- were generally higher at the LFS than at the SFS (Table 2). The highest concentrations of NH_4^+ were generally associated with periods of standing water (LFS; March 2014/2015) or immediately after (SFS; March 2014) the disappearance of standing water (Table 2 and Fig. 3c). For NO_3^- the highest concentrations were generally found at the LFS, but there was no discernible pattern over the ∼ 2 years of the study at either the LFS or SFS.

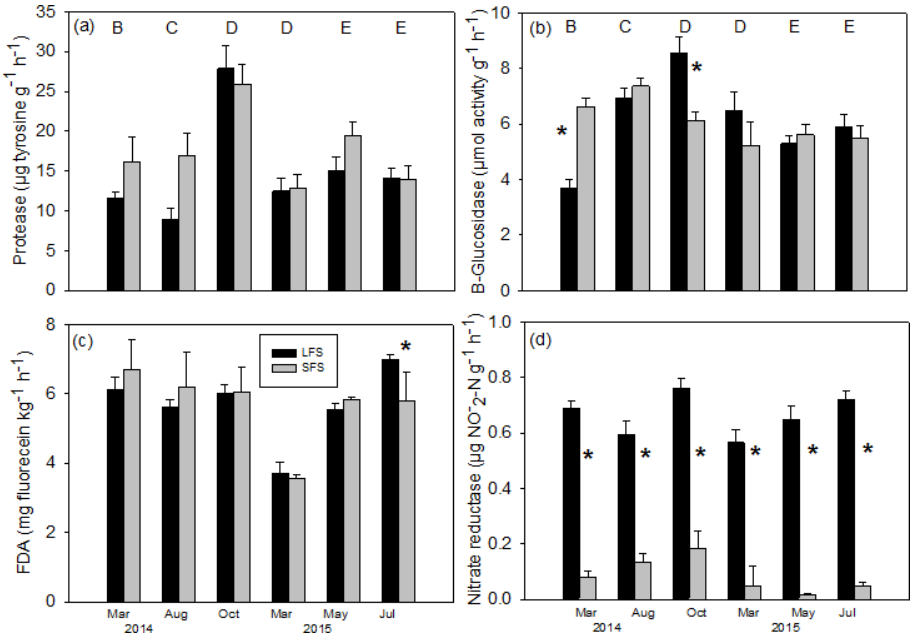

Figure 6. Soil enzymatic activities of **(a)** protease, **(b)** beta-glucosidase, **(c)** fluorescein diacetate and **(d)** nitrate reductase measured at different sampling dates from the LFS and SFS. Periods corresponding to different sampling dates are indicated by different letters (see Fig. 3). Values are mean ± SE ($n = 4$–6). Asterisks indicate a significant difference between the LFS and SFS for the same sampling date at ($P < 0.05$).

3.7 Plant biomass

The values for aboveground plant biomass were approximately 6 times higher at the SFS (35.51 Mg ha^{-1}) compared to the LFS (6.02 Mg ha^{-1}).

4 Discussion

The mean annual CO_2 emissions were 11.37 and 8.47 Mg CO_2–C ha^{-1} yr^{-1} from the LFS and SFS, respectively. Longer-term flooding therefore increased, rather than reduced, the annual emissions by approximately 40 % and suggests that any increase in freshwater flooding in response to climate change could result in a significant increase in carbon dioxide emissions from these systems. The annual emissions of CO_2 found in this study are in line with those previously reported for floodplain wetlands (10.91 ± 0.54 Mg CO_2–C ha^{-1} yr^{-1}) (Batson et al., 2015), coastal plain wetlands (11.29 Mg CO_2–C ha^{-1} yr^{-1}) (Morse et al., 2012) and occasionally (9.7 Mg CO_2–C ha^{-1} yr^{-1}) or frequently flooded (13 Mg CO_2–C ha^{-1} yr^{-1}) riparian forests (Jacinthe, 2015). Our results are also in part agreement with other investigations on comparable ecosystems that examined the impact of flooding on GHGs (Morse et al., 2012; Jacinthe, 2015; Kim et al., 2015; Marín-Muñiz et al., 2015). Jacinthe (2015) reported that CO_2 fluxes during summer were larger from a riparian forest affected by floods in winter and spring than from a flood protected area. Similarly, Morse et al. (2012) found higher rates of CO_2 emission in the dry period from short and intermittently flooded restored wetland habitats compared to both permanently flooded and unflooded sites.

4.1 Relationships between CO_2 emissions and water and nutrient availability

The overall negative relationship between CO_2 emissions and soil moisture (Fig. 5b) suggests that flooding or high soil water availability impedes the decomposition processes that lead to CO_2 production via the creation of low-oxygen conditions. Standing water would also act as an additional constraint on annual emissions by acting as a physical barrier to gaseous diffusion. However, somewhat paradoxically, larger annual CO_2 emissions were associated with the LFS site, i.e. the site inundated for longer. However, the highest CO_2 emissions *and* the period when the differences in CO_2 emissions between the two sites were greatest occurred in the summer season after the disappearance of standing water, when the soil was better oxygenated (Fig. 3d). Potentially, the presence of standing water during the autumn/winter months could inhibit CO_2 emissions at the LFS by acting as a gaseous barrier. However, the values found for the SFS for the same period are similar, indicating that this is unlikely to have a significant impact on the annual emissions. Reductions in mineralisation caused by low temperatures may be the more significant factor at these times of the year, consistent with the strong correlations between CO_2 emissions and temperature

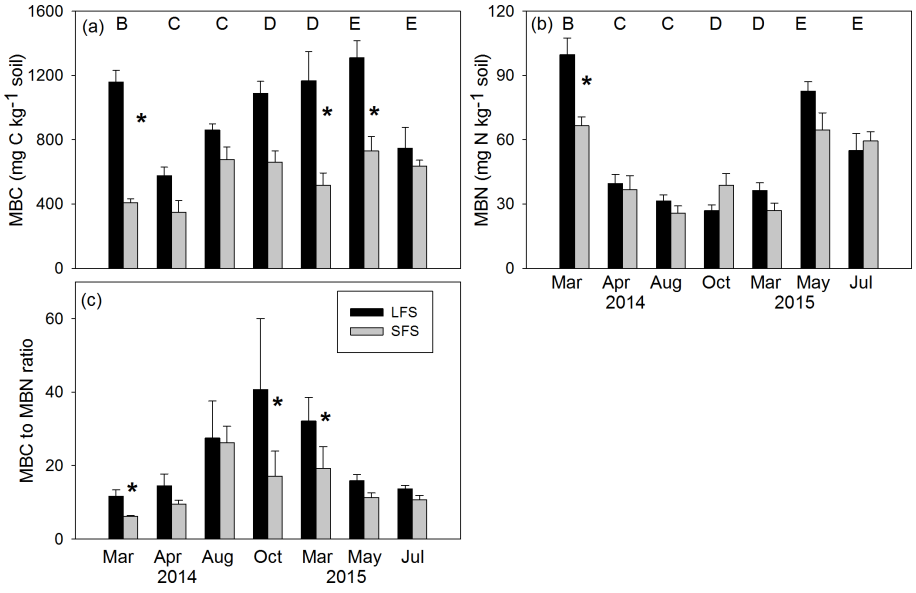

Figure 7. Seasonal variations in **(a)** MBC, **(b)** MBN and **(c)** MBC : MBN from the LFS and SFS measured at different sampling dates. Periods corresponding to different sampling dates are indicated by different letters (see Fig. 3). Vertical bars represent the standard errors of the mean ($n = 4$–6). Asterisks indicate a significant difference between the LFS and SFS for the same sampling date ($P < 0.05$).

Table 2. Mean ± SE of soil NH_4^+ and NO_3^- concentrations at 0–5 cm depths (mg N kg^{-1}) for different sampling dates in 2014 and 2015.

Date (period)	LFS		SFS	
	NH_4^+	NO_3^-	NH_4^+	NO_3^-
4 March 2014 (B)	30.49 ± 3.79	0.99 ± 0.08	25.63 ± 1.85	0.52 ± 0.15
30 April 2014 (C)	12.93 ± 4.36	0.30 ± 0.06	4.37 ± 0.80	0.00 ± 0.00
19 August 2014 (C)	12.47 ± 1.12	0.28 ± 0.11	16.85 ± 1.67	0.29 ± 0.17
8 March 2015 (D)	25.80 ± 2.37	0.00 ± 0.00	17.66 ± 0.84	0.00 ± 0.00
28 May 2015 (E)	18.24 ± 2.28	2.28 ± 0.79	15.88 ± 1.36	0.12 ± 0.11
17 July 2015 (E)	13.08 ± 0.41	0.51 ± 0.13	12.11 ± 0.36	0.24 ± 0.15

that were observed in this study. This observation implies that the impact of flooding on annual CO_2 emissions could therefore be strongly sensitive to the intra-annual timing of flooding events.

Higher CO_2 emissions were obtained at the LFS during the drier parts of the year, when there were similar values for soil moisture/soil temperature at both sites. This may be related to higher organic matter content and nutrient status and a generally higher microbial biomass at the LFS. Compared to soils supplied with no or little organic matter/nutrients, soils that have received more organic matter are likely to emit substantially larger amounts of CO_2 (Winton and Richardson, 2015). The availability of organic matter is one of the most important factors controlling the production of GHGs in wetlands (Badiou et al., 2011). The source of the organic matter will be dependent on the hydrological connectivity of the wetland to the upstream land use system in addition to plant litter derived from wetland plants (Hernandez and Mitsch, 2007). Based on the plant biomass estimates (Sect. 3.7), similar or even higher carbon contents would have been expected for the SFS had the carbon been contributed mainly from the plant community. The difference in total C and N values between the LFS and SFS sites and, specifically, the rapid decline in these nutrients down through the soil profile indicate these are derived largely from external sources, rather than produced in situ, from plant-related material. These nutrients were presumably introduced with the drainage water. Many studies have reported an increase in the release of CO_2 via soil respiration as a result of the increased input of organic matter, particularly in wetlands (Samaritani et al., 2011; Winton and Richardson, 2015). Given that the C fluxes observed in this work are determined largely by external nutrient inputs, this adds to the growing body of evidence that biogeochemical processes, including greenhouse gas emissions, in floodplain wetlands are predominantly determined by off-site/catchment-related events (Batson et al., 2015).

4.2 Relationship between CO_2 fluxes and soil temperature

There was a positive relationship between temperature and CO_2 production at the two sites. Temperature was the single most important variable overall explaining variations in CO_2 emissions. Kim et al. (2015) also showed that CO_2 production increased with rising temperature from incubated flooded and non-flooded boreal soils. Variations in CO_2 emissions frequently matched changes in temperature at times when other variables, such as soil moisture, were invariant, most obviously over the duration of period D (Fig. 4a, c and d). As soil temperature was essentially identical between the sites at any given time the different relationships between soil temperature and CO_2 emissions (Fig. 5a) imply that at least one other variable is involved. The greater abundance of soil carbon and nitrogen, accompanied by a generally higher microbial biomass suggests substrate availability at the LFS was greater for soil microbial processes (Wang et al., 2003). The higher Q_{10} values at the LFS (2.49) compared to the SFS (2.08) also suggest differences in the microbial populations at the two sites. The higher Q_{10} values for CO_2 emissions at the LFS indicates that longer-term flooded sites could be more sensitive to climate-change-related warming (Zhou et al., 2014).

4.3 Effect of redox potential on soil CO_2 and N_2O fluxes

The weak correlation between redox potential and CO_2 emissions, as well as the absence of a relationship with N_2O fluxes (Sect. 3.4) for both sites, suggests soil redox potential had minimal influence on the emissions of either gas. This contrasts with the finding of Marín-Muñiz et al. (2015), who identified redox potential and water level as the main factors controlling GHG emissions in coastal freshwater wetlands.

The redox potential of the two sites was different and the highest CO_2 emissions occurred at 220–362 and 145–259 mv at the SFS and LFS, respectively. These data do not imply that larger CO_2 fluxes reflect more oxidised soil conditions. The redox level of the soil is not critical as the highest CO_2 emissions at the LFS actually occurred in the lower end of the above range of redox values. The redox potential at the LFS increases markedly and then remains constant, soon after the disappearance of standing water, whilst there was no immediate response in terms of CO_2 emissions. Even at times (periods C and E) when soil moisture contents are identical between the sites, CO_2 emissions were higher at the LFS and redox values lower, which could be due to the higher organic matter content at the LFS. Gardiner and James (2012) showed a marked decrease in redox potential (more negative) as a result of organic matter addition in their wet soil microcosm study. However, the redox status of soil is also controlled by the availability of electron acceptors and microbial activity (Oktyabrskii and Smirnova, 2012; Hunting and Kampfraath, 2013).

No particular redox range was confidently identified as being associated with greater N_2O emissions. The fluxes were somewhat higher when the redox value was above 249 mv at the SFS and between −232 and 228 mv at the LFS. Similarly, many previous studies have reported higher N_2O emissions in flood-affected wetlands across a wide range of redox potentials (−100 to 430 mv) (Yu et al., 2001; Wlodarczyk et al., 2003; Morse et al., 2012). Marín-Muñiz et al. (2015) found an optimum range of 100–360 mv for the reduction of nitrate to N_2O from a coastal wetland, whereas Morse et al. (2012) reported values of 89 and 5.3 mv from rarely and intermittently flooded areas, respectively, as the conditions conducive for N_2O production.

4.4 Relationship between water depth and CO_2 and N_2O fluxes

The greater water depths at the LFS during flooding were accompanied by a decrease in the rate of CO_2 emissions, perhaps due to a combination of diffusional constraints and decreased oxygen availability, as a result of higher standing water levels. Water depth has been shown to be more significant than temperature in determining the variation in CO_2 fluxes during inundation (Dixon et al., 2014). Multiple regression analysis of CO_2 fluxes with water depth and soil temperature combined showed a significant paraboloid relationship ($R^2 = 0.62$, $P < 0.001$) (Fig. 8) but most of this variation was explained by changes in water depth alone ($R^2 = 0.45$, $P < 0.001$) (Fig. 5c). Peak CO_2 fluxes (above 75 mg CO_2–C m^{-2} h^{-2}) were recorded during periods B and D when water depths less than 9 cm were coupled with soil temperatures above 11 °C. No major variations in CO_2 fluxes were observed when water depths exceeded 12 cm. Other studies have shown a significant relationship between N_2O fluxes and water depth in riparian woodlands (Mander et al., 2015; Marín-Muñiz et al., 2015), but no such correlation was found in this study (Sect. 3.4). Audet et al. (2013) also found no significant impact of water depth on N_2O emission from a temperate riparian wetland.

4.5 N_2O fluxes and their controlling factors

No relationship was found between N_2O fluxes and soil moisture content or temperature at the LFS and only a weak relationship at the SFS, suggesting the influence of these variables on nitrification and denitrification processes leading to N_2O production from these sites is limited. Several other environmental factors such as pH, oxygen concentration and nitrogen availability are known to affect the production of N_2O (Ullah and Zinati, 2006; Van den Heuvel et al., 2011; Burgin and Groffman, 2012). In this study, the lower pH, as well as a higher nitrogen availability and higher MBC at the LFS, would be expected to favour N_2O emissions (Liu

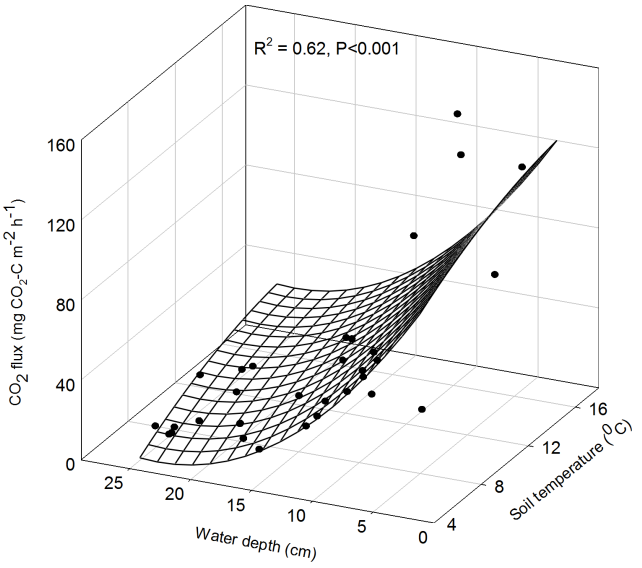

Figure 8. Dependence of CO_2 fluxes on water depth and soil temperature during the intervals in which the LFS is flooded. A significant ($R^2 = 0.62$, $P < 0.001$) 3-D paraboloid regression is shown in the mesh plot. Individual values shown are means ($n = 3$–4).

et al., 2010; Van den Heuvel et al., 2011). However, apart from the constantly positive and higher N_2O fluxes observed at the LFS for many of the sampling dates in period D, no appreciable differences in N_2O emission were detected between the two sites. The generally higher N_2O emissions from the LFS in period D might be associated with the persistent anaerobic conditions that would have favoured a transient reduction of NO_3^- to N_2O. Higher soil NH_4^+ concentrations under largely anoxic conditions (periods A, B and D) and its progressive decrease through the aerobic period (periods C and E) in both sites (Table 2) indicate increased nitrification and ammonia oxidation that may lead to N_2O production as aeration of soil and gas diffusion improves (Firestone and Davidson, 1989). This is a potential explanation for the larger N_2O emissions observed at the SFS during the larger part of the first and, on a few occasions, during the second summer period (periods C and E). Continuous and relatively low, or negative, N_2O emissions were observed for both sites during the early part of periods C and E (i.e. after draining of the flood water at the LFS). This is most likely due to increased uptake of N by growing vegetation that reduces the amount of inorganic N available for conversion to N_2O and offsetting any tendency for the increase in soil aeration to promote N_2O formation. This potentially also explains the absence of N_2O fluxes of a similar magnitude at the LFS during the summer where, unlike at the SFS, the immediate development and recovery of grasses was likely impeded by the preceding episode of prolonged waterlogging (Steffens et al., 2005).

The annual N_2O emissions estimated in this work are within the range of emissions obtained in restored temperate wetlands in Denmark and the Netherlands (Hefting et al., 2003; Audet et al., 2013). Fisher et al. (2014) reported higher annual N_2O emissions (4.32 kg N_2O–N ha^{-1}) from flood prone riparian buffer zones in Indiana, USA, compared to unflooded buffer zones (1.03 kg N_2O–N ha^{-1}).

In terms of the contribution of each gas to the GWP, expressed as CO_2 equivalents, N_2O contributed only 16 % to GWP, which is low compared to the CO_2 contribution (84 %). We have not assessed the contribution of CH_4 emissions, which are often a major GHG in permanently inundated soils. Whilst other studies of floodplains and freshwater wetlands do report a high contribution of methane to the GWP (Altor and Mitsch, 2006; Koh et al., 2009), this may not always be the case. For instance, Jacinthe (2015) showed that some terrestrial riparian ecosystems, which were exposed to variable flooding frequencies, routinely acted as a strong sink for CH_4, except for a small contribution in emissions from permanently flooded sites. In many ecosystems where flooding is intermittent or periodic and of a shallow depth, CO_2 is the dominant gaseous flux (e.g. Altor and Mitsch, 2006; Jerman et al., 2009; Morse et al., 2012; Batson et al., 2015; Jacinth, 2015; Winton and Richardson, 2015). For example, Morse et al. (2012) showed that CO_2 fluxes comprised 60 to 100 % of the contribution (8000–64 800 kg CO_2 ha^{-1} yr^{-1}) to the total GHG emissions from an intermittently and permanently flooded coastal plain; in contrast, CH_4 fluxes ranged from −6.87 to 197 kg CH_4 ha^{-1} yr^{-1}. The highest emissions of CH_4 were from the permanently flooded site. Broadly similar findings were reported by Batson et al. (2015), where CH_4 made no contribution to the total GHG emissions from floodplain areas with contrasting hydroperiods. As the major period of flooding also occurred during the cooler period of the year, the lower temperatures would have inhibited CH_4 emissions.

5 Conclusions

This study provides evidence that the interaction between a grassland ecosystem and its hydrologic regime impacts on the annual emissions of greenhouse gases. Flooding duration affected the dynamics of CO_2 and, to a lesser extent, N_2O fluxes. The emissions of CO_2 were higher with longer-term (∼ 6 months) compared to shorter-term (∼ 2–4 weeks) flooding. Temperature and soil water content are identified as the most important factors controlling the seasonal pattern of the CO_2 fluxes, especially for the longer-term flooded site. The higher emissions from the longer-term flooded site are likely linked to the higher inputs of organic materials/nutrients and associated increases in microbial biomass and, possibly, to changes in the microbial populations. In contrast, no individual environmental parameter, or any combination of them, was found to have a major influence on the emissions of N_2O. However, flooding enhanced N_2O production during the period in which water was standing on the longer-term flooded

site, likely due to enhanced denitrification. The controlling mechanisms underpinning the observed N_2O fluxes are not clear. However, based on the information obtained from the current study the contribution of N_2O emissions to global warming in these ecosystems would be minimal. A more extensive study of the effect of specific hydrologic patterns (flooding frequency, timing and duration) on the dynamics of GHGs, including CH_4, would be required to better assess the global warming potential of flood-affected ecosystems.

Data availability. Data are available on request by contacting the corresponding author.

Competing interests. The authors declare that they have no conflict of interest.

Acknowledgements. This project is part of the Earth and Natural Sciences Doctoral Studies Programme, which is funded by the Higher Education Authority (HEA) through the Programme for Research at Third Level Institutions, Cycle 5 (PRTLI-5), and is co-funded by the European Regional Development Fund (ERDF). We wish to thank BirdWatch Ireland in Wicklow for providing the study site for this research and their support during the process of site formation. We thank the Associate Editor and reviewers for their constructive comments.

Edited by: A. Ito
Reviewed by: T. K. Yoon and one anonymous referee

References

Alongi, D. M., Tirendi, F., Dixon, P., Trott, L. A., and Brunskill, G. J.: Mineralization of Organic Matter in Intertidal Sediments of a Tropical Semi-enclosed Delta, Estuar. Coast. Shelf S., 48, 451–467, 1999.

Altor, A. E. and Mitsch, W. J.: Methane flux from created riparian marshes: Relationship to intermittent versus continuous inundation and emergent macrophytes, Ecol. Eng., 28, 224–234, 2006.

Altor, A. E. and Mitsch, W. J.: Pulsing hydrology, methane emissions and carbon dioxide fluxes in created marshes: A 2-year ecosystem study, Wetlands, 28, 423–438, doi:10.1672/07-98.1, 2008.

Audet, J., Elsgaard, L., Kjaergaard, C., Larsen, S. E., and Hoffmann, C. C.: Greenhouse gas emissions from a Danish riparian wetland before and after restoration, Ecol. Eng., 57, 170–182, 2013.

Badiou, P., McDougal, R., Pennock, D., and Clark, B.: Greenhouse gas emissions and carbon sequestration potential in restored wetlands of the Canadian prairie pothole region, Wetlands Ecol. Manag., 19, 237–256, doi:10.1007/s11273-011-9214-6, 2011.

Bateman, E. J. and Baggs, E. M.: Contributions of nitrification and denitrification to N_2O emissions from soils at different water-filled pore space, Biol. Fertil. Soils, 41, 379–388, doi:10.1007/s00374-005-0858-3, 2005.

Batson, J., Noe, G. B., Hupp, C. R., Krauss, K. W., Rybicki, N. B., and Schenk, E. R.: Soil greenhouse gas emissions and carbon budgeting in a short-hydroperiod floodplain wetland, J. Geophys. Res.-Biogeo., 120, 77–95, doi:10.1002/2014JG002817, 2015.

Beniston, M., Stephenson, D. B., Christensen, O. B., Ferro, C. A. T., Frei, C., Goyette, S., Halsnaes, K., Holt, T., Jylhä, K., Koffi, B., Palutikof, J., Schöll, R., Semmler, T., and Woth, K.: Future extreme events in European climate: an exploration of regional climate model projections, Climatic Change, 81, 71–95, doi:10.1007/s10584-006-9226-z, 2007.

Bossio, D. A. and Scow, K. M.: Impacts of Carbon and Flooding on Soil Microbial Communities: Phospholipid Fatty Acid Profiles and Substrate Utilization Patterns, Microb. Ecol., 35, 265–278, doi:10.1007/s002489900082, 1998.

Brookes, P. C., Landman, A., Pruden, G., and Jenkinson, D.: Chloroform fumigation and the release of soil nitrogen: a rapid direct extraction method to measure microbial biomass nitrogen in soil, Soil Biol. Biochem., 17, 837–842, 1985.

Burgin, A. J. and Groffman, P. M.: Soil O_2 controls denitrification rates and N_2O yield in a riparian wetland, J. Geophys. Res.-Biogeo., 117, G01010, doi:10.1029/2011JG001799, 2012.

Butterbach-Bahl, K., Baggs, E. M., Dannenmann, M., Kiese, R., and Zechmeister-Boltenstern, S.: Nitrous oxide emissions from soils: how well do we understand the processes and their controls?, Philos. T. R. Soc. B., 368, 20130122, doi:10.1098/rstb.2013.0122, 2013.

Christensen, J. and Christensen, O.: A summary of the PRUDENCE model projections of changes in European climate by the end of this century, Climatic Change, 81, 7–30, doi:10.1007/s10584-006-9210-7, 2007.

Davidson, E. A. and Janssens, I. A.: Temperature sensitivity of soil carbon decomposition and feedbacks to climate change, Nature, 440, 165–173, doi:10.1038/nature04514, 2006.

Dixon, S. D., Qassim, S. M., Rowson, J. G., Worrall, F., Evans, M. G., Boothroyd, I. M., and Bonn, A.: Restoration effects on water table depths and CO_2 fluxes from climatically marginal blanket bog, Biogeochemistry, 118, 159–176, doi:10.1007/s10533-013-9915-4, 2014.

Doornkamp, J. C.: Coastal flooding, global warming and environmental management, J. Environ. Manage., 52, 327–333, 1998.

Eivazi, F. and Tabatabai, M. A.: Glucosidases and galactosidases in soils, Soil Biol. Biochem., 20, 601–606, 1988.

Firestone, M. K. and Davidson, E. A.: Microbiological basis of NO and N_2O production and consumption in soil, in: Exchange of trace gases between terrestrial ecosystems and the atmosphere, Wiley, New York, NY, 47, 7–21, 1989.

Fisher, K., Jacinthe, P., Vidon, P., Liu, X., and Baker, M.: Nitrous oxide emission from cropland and adjacent riparian buffers in contrasting hydrogeomorphic settings, J. Environ. Qual., 43, 338–348, doi:10.2134/jeq2013.06.0223, 2014.

Gardiner, D. T. and James, S.: Wet Soil Redox Chemistry as Affected by Organic Matter and Nitrate, Am. J. Climate Change, 1, 205–209, 10.4236/ajcc.2012.14017, 2012.

Gee, G. W. and Bauder, J. W.: Particle-size analysis1, in: Methods of Soil Analysis. Part 1-Physical and Mineralogical Methods, edited by: Klute, A., SSSA, ASA, Madison, WI., 383–411, 1986.

Glatzel, S., Basiliko, N., and Moore, T.: Carbon dioxide and methane production potentials of peats from

natural, harvested and restored sites, eastern Québec, Canada, Wetlands, 24, 261–267, doi:10.1672/0277-5212(2004)024[0261:CDAMPP]2.0.CO;2, 2004.

Green, V. S., Stott, D. E., and Diack, M.: Assay for fluorescein diacetate hydrolytic activity: Optimization for soil samples, Soil Biol. Biochem., 38, 693–701, 2006.

Hansen, M., Clough, T. J., and Elberling, B.: Flooding-induced N_2O emission bursts controlled by pH and nitrate in agricultural soils, Soil Biol. Biochem., 69, 17–24, 2014.

Hefting, M. M., Bobbink, R., and de Caluwe, H.: Nitrous oxide emission and denitrification in chronically nitrate-loaded riparian buffer zones, J. Environ. Qual., 32, 1194–1203, doi:10.2134/jeq2003.1194, 2003.

Hernandez, M. E. and Mitsch, W. J.: Denitrification Potential and Organic Matter as Affected by Vegetation Community, Wetland Age, and Plant Introduction in Created Wetlands, J. Environ. Qual., 36, 333–342, doi:10.2134/jeq2006.0139, 2007.

Hunting, E. R. and Kampfraath, A. A.: Contribution of bacteria to redox potential (E_h) measurements in sediments, Int. J. Environ. Sci. Technol., 10, 55–62, doi:10.1007/s13762-012-0080-4, 2013.

IPCC: Summary for Policymakers, in: Climate Change 2007: The Physical Science Basis, Contribution of Working Group I to the Fourth Assessment Report of the Intergovernmental Panel on Climate Change, edited by: Solomon, S. D., Qin, D., Manning, M. R., Chen, Z., Marquis, M., Averyt, K. B., Tignor, M., and Miller, H. L., Cambridge University Press, Cambridge, UK and New York, NY, USA, 996 pp., 2007.

Jacinthe, P., Bills, J., Tedesco, L., and Barr, R.: Nitrous oxide emission from riparian buffers in relation to vegetation and flood frequency, J. Environ. Qual., 41, 95–105, doi:10.2134/jeq2011.0308, 2012.

Jacinthe, P. A.: Carbon dioxide and methane fluxes in variably-flooded riparian forests, Geoderma, 241–242, 41–50, 2015.

Jerman, V., Metje, M., Mandic-Mulec, I., and Frenzel, P.: Wetland restoration and methanogenesis: the activity of microbial populations and competition for substrates at different temperatures, Biogeosciences, 6, 1127–1138, doi:10.5194/bg-6-1127-2009, 2009.

Jonasson, S., Michelsen, A., Schmidt, I. K., Nielsen, E. V., and Callaghan, T. V.: Microbial biomass C, N and P in two arctic soils and responses to addition of NPK fertilizer and sugar: implications for plant nutrient uptake, Oecologia, 106, 507–515, doi:10.1007/BF00329709,1996.

Juutinen, S., Alm, J., Martikainen, P., and Silvola, J.: Effects of spring flood and water level draw-down on methane dynamics in the littoral zone of boreal lakes, Freshwater Biol., 46, 855-869, doi:10.1046/j.1365-2427.2001.00721.x, 2001.

Kandeler, E., Luxhøi, J., Tscherko, D., and Magid, J.: Xylanase, invertase and protease at the soil–litter interface of a loamy sand, Soil Biol. Biochem., 31, 1171–1179, 1999.

Kim, Y., Ullah, S., Roulet, N. T., and Moore, T. R.: Effect of inundation, oxygen and temperature on carbon mineralization in boreal ecosystems, Sci. Total Environ., 511, 381–392, 2015.

Kirwan, M. L., Guntenspergen, G. R., and Langley, J. A.: Temperature sensitivity of organic-matter decay in tidal marshes, Biogeosciences, 11, 4801–4808, doi:10.5194/bg-11-4801-2014, 2014.

Koh, H.-S., Ochs, C. A., and Yu, K.: Hydrologic gradient and vegetation controls on CH_4 and CO_2 fluxes in a spring-fed forested wetland, Hydrobiologia, 630, 271–286, doi:10.1007/s10750-009-9821-x, 2009.

Lewis, D. B., Brown, J. A., and Jimenez, K. L.: Effects of flooding and warming on soil organic matter mineralization in *Avicennia germinans* mangrove forests and *Juncus roemerianus* salt marshes, Estuar. Coast. Shelf S., 139, 11–19, 2014.

Li, X., Hou, L., Liu, M., Lin, X., Li, Y., and Li, S.: Primary effects of extracellular enzyme activity and microbial community on carbon and nitrogen mineralization in estuarine and tidal wetlands, Appl. Microbiol. Biotechnol., 99, 2895–2909, doi:10.1007/s00253-014-6187-4, 2015.

Liu, B., Mørkved, P. T., Frostegård, Å., and Bakken, L. R.: Denitrification gene pools, transcription and kinetics of NO, N_2O and N_2 production as affected by soil pH, FEMS Microbiol. Ecol., 72, 407–417, doi:10.1111/j.1574-6941.2010.00856.x, 2010.

Maag, M. and Vinther, F. P.: Nitrous oxide emission by nitrification and denitrification in different soil types and at different soil moisture contents and temperatures, Appl. Soil Ecol., 4, 5–14, 1996.

Machefert, S. E. and Dise, N. B.: Hydrological controls on denitrification in riparian ecosystems, Hydrol. Earth Syst. Sci., 8, 686–694, doi:10.5194/hess-8-686-2004, 2004.

Mander, Ü., Maddison, M., Soosaar, K., Teemusk, A., Kanal, A., Uri, V., and Truu, J.: The impact of a pulsing groundwater table on greenhouse gas emissions in riparian grey alder stands, Environ. Sci. Pollut. Res., 22, 2360–2371, doi:10.1007/s11356-014-3427-1, 2015.

Marín-Muñiz, J. L., Hernández, M. E., and Moreno-Casasola, P.: Greenhouse gas emissions from coastal freshwater wetlands in Veracruz Mexico: Effect of plant community and seasonal dynamics, Atmos. Environ., 107, 107–117, 2015.

McNicol, G. and Silver, W. L.: Separate effects of flooding and anaerobiosis on soil greenhouse gas emissions and redox sensitive biogeochemistry, J. Geophys. Res.-Biogeo., 119, 557–566, doi:10.1002/2013JG002433, 2014.

Morse, J. L., Ardón, M., and Bernhardt, E. S.: Greenhouse gas fluxes in southeastern U.S. coastal plain wetlands under contrasting land uses, Ecol. Appl., 22, 264–280, doi:10.1890/11-0527.1, 2012.

Noe, G., Hupp, C., and Rybicki, N.: Hydrogeomorphology Influences Soil Nitrogen and Phosphorus Mineralization in Floodplain Wetlands, Ecosystems, 16, 75-94, doi:10.1007/s10021-012-9597-0, 2013.

Oelbermann, M. and Schiff, S. L.: Quantifying Carbon Dioxide and Methane Emissions and Carbon Dynamics from Flooded Boreal Forest Soil, J. Environ. Qual., 37, 2037–2047, doi:10.2134/jeq2008.0027, 2008.

Oktyabrskii, O. N. and Smirnova, G. V.: Redox potential changes in bacterial cultures under stress conditions, Microbiology+, 81, 131-142, doi:10.1134/S0026261712020099, 2012.

Peralta, A. L., Ludmer, S., and Kent, A. D.: Hydrologic history influences microbial community composition and nitrogen cycling under experimental drying/wetting treatments, Soil Biol. Biochem., 66, 29–37, 2013.

Rinklebe, J. and Langer, U.: Microbial diversity in three floodplain soils at the Elbe River (Germany), Soil Biol. Biochem., 38, 2144–2151, 2006.

Samaritani, E., Shrestha, J., Fournier, B., Frossard, E., Gillet, F., Guenat, C., Niklaus, P. A., Pasquale, N., Tockner, K., Mitchell,

E. A. D., and Luster, J.: Heterogeneity of soil carbon pools and fluxes in a channelized and a restored floodplain section (Thur River, Switzerland), Hydrol. Earth Syst. Sci., 15, 1757–1769, doi:10.5194/hess-15-1757-2011, 2011.

Schnürer, J. and Rosswall, T.: Fluorescein diacetate hydrolysis as a measure of total microbial activity in soil and litter, Appl. Environ. Microbiol., 43, 1256–1261, 1982.

Smith, K., Ball, T., Conen, F., Dobbie, K., Massheder, J., and Rey, A.: Exchange of greenhouse gases between soil and atmosphere: interactions of soil physical factors and biological processes, Eur. J. Soil Sci., 54, 779–791, doi:10.1046/j.1351-0754.2003.0567.x, 2003.

Steffens, D., Hütsch, B., Eschholz, T., Lošák, T., and Schubert, S.: Water logging may inhibit plant growth primarily by nutrient deficiency rather than nutrient toxicity, Plant Soil Environ., 51, 545–552, 2005.

Ullah, S. and Zinati, G.: Denitrification and nitrous oxide emissions from riparian forests soils exposed to prolonged nitrogen runoff, Biogeochemistry, 81, 253–267, doi:10.1007/s10533-006-9040-8, 2006.

Unger, I. M., Kennedy, A. C., and Muzika, R.-M.: Flooding effects on soil microbial communities, Appl. Soil Ecol., 42, 1–8, 2009.

Vance, E., Brookes, P., and Jenkinson, D.: An extraction method for measuring soil microbial biomass C, Soil Biol. Biochem., 19, 703–707, 1987.

Van den Heuvel, R., Bakker, S., Jetten, M., and Hefting, M.: Decreased N_2O reduction by low soil pH causes high N_2O emissions in a riparian ecosystem, Geobiology, 9, 294–300, doi:10.1111/j.1472-4669.2011.00276.x, 2011.

Van Der Heijden, M. G. A., Bardgett, R. D., and Van Straalen, N. M.: The unseen majority: soil microbes as drivers of plant diversity and productivity in terrestrial ecosystems, Ecol. Lett., 11, 296–310, doi:10.1111/j.1461-0248.2007.01139.x, 2008.

Wang, W. J., Dalal, R. C., Moody, P. W., and Smith, C. J.: Relationships of soil respiration to microbial biomass, substrate availability and clay content, Soil Biol. Biochem., 35, 273–284, 2003.

Wilson, J. S., Baldwin, D. S., Rees, G. N., and Wilson, B. P.: The effects of short-term inundation on carbon dynamics, microbial community structure and microbial activity in floodplain soil, River Res. Appl., 27, 213–225, doi:10.1002/rra.1352, 2011.

Winton, R. S. and Richardson, C.: The Effects of Organic Matter Amendments on Greenhouse Gas Emissions from a Mitigation Wetland in Virginia's Coastal Plain, Wetlands, 35, 969–979, doi:10.1007/s13157-015-0674-y, 2015.

Wlodarczyk, T., Stêpniewska, Z., and Brzezinska, M.: Denitrification, organic matter and redox potential transformations in Cambisols, Int. Agrophysics, 17, 219–227, 2003.

Yu, K., Wang, Z., Vermoesen, A., Patrick Jr., W., and Van Cleemput, O.: Nitrous oxide and methane emissions from different soil suspensions: effect of soil redox status, Biol. Fert. Soils, 34, 25–30, doi:10.1007/s003740100350, 2001.

Zhou, W., Hui, D., and Shen, W.: Effects of soil moisture on the temperature sensitivity of soil heterotrophic respiration: a laboratory incubation study, PLoS ONE, 9, e92531, doi:10.1371/journal.pone.0092531, 2014.